Seismic response analysis of high-speed railway vehicle-slab ballastless track-bridge system under near-fault pulse ground motions

2014 NZSEE Conference

L. K. Chen

College of Civil Science and Engineering, Yangzhou University, China

National Engineering Laboratory for High-Speed Railway Construction, Central South University, China

L. Z. Jiang & Z. P. Zeng

School of Civil Engineering, Central South University, China

National Engineering Laboratory for High-Speed Railway Construction, Central South University, China

G. W. Chen

Department of Civil and Environmental Engineering, University of Auckland, New Zealand

ABSTRACT: This paper presents a finite element method (FEM) framework for the dynamic analysis of coupled vehicle—bridge systems under near- field /far-field ground motions. A train car with two bogies is assumed to be represented sufficiently by a discrete, rigid multi-body system with thirty-eight degrees of freedoms (DOFs). The normal Hertzian contact theory and the tangential Kalker linear theory modified by the Shen-Hedrick-Elkins theory is used to establish the dynamic wheel-rail interaction relationship. The triple layered ballastless slab-track is being introduced into the high-speed vehicle-bridge system. Based on the PEER Ground Motion Database, TTBDA, a computer program for the simulation of a high-speed train running on the railway structure under seismic loads, has been developed. The seismic responses of the vehicle-bridge system are calculated, and the impact of the near-fault effect on the dynamic responses of the vehicle-bridge system are studied. The case study results demonstrate that near-fault pulse-like ground motions more significantly affect the dynamic responses of the bridge and the running safety of the trains than the nonpulse-like motions of far-field ground motions.

1 INTRODUCTION

It is well-known that near-field ground motions can severely impact and can potentially destroy urban infrastructure when the causative fault is in the immediate vicinity of a large metropolitan area, as demonstrated by earthquakes such as the 1971 San Fernando, 1989 Loma Prieta, 1994 Northridge, 1995 Hyogoken-Nanbu (Kobe), 1999 Kocaeli and 1999 Chi-Chi earthquake. Those near-field ground motions are characterized by a significant velocity pulse effect, which exposes structures to high input energy at the beginning of the record.

The influence of pulse-like, near-field ground motions on the seismic response of structures has become a crucial research topic in high-speed railway design. High-speed railways have more stringent design requirements than conventional railways, because they need to have a large curve radius and a fully-closed operation to ensure a smooth track and safety and stability while running trains. These strict design requirements for high-speed railways result in many more bridges than conventional railways, which greatly increases the likelihood that trains will be located on bridges when an earthquake strikes. Elevated bridges can stretch for dozens of kilo-meters. For example, the

Beijing-Shanghai high-speed railway is 1,318 km long and includes 244 bridges occupying 1,059.4 km, meaning that 80.5% of the total length of the railway is composed of bridges. Therefore, the seismic analysis of coupled bridge-train systems during earthquakes is imperative to ensure the safety of vehicles and to minimize the loss of human lives, thereby preventing accidents such as the recent derailment during the Niigata Earthquake on 23 October 2004.

Many researchers have studied the dynamic behaviour of train-bridge coupling systems and the aseismic design of bridges. Yang and Wu [1] carried out a dynamic response analysis of train-bridge systems subjected to uniform seismic ground motions. Xia et al. [2] and Du et al. [3] presented a framework for the dynamic analysis of train-bridge systems subjected to seismic ground motions with the wave passage effect. Miyamoto et al. have published studies on the dynamic responses of the Shinkansen train-bridge systems to seismic excitations [4].

While there have been numerous studies evaluating the seismic performance of vehicle-bridge systems under earthquake conditions, there are some questions regarding the method of seismic analysis of vehicle-bridge systems. First, few studies have considered the unique challenges of building vehicle-bridge systems in near-field regions, as near-field seismic ground motions differ from typical far-field ground motions by having frequent pulses of intense velocity for relatively long periods. Second, the moving loads model, or the equidistant moving oscillators model, may limit the practical application of the vehicle-bridge system. Third, existing research on seismic analysis of the vehicle-bridge system has not studied the influence of a slab ballastless track system or considered it as an extra-mass, and the constraints that the slab ballastless track imposes cannot be ignored [5].

This paper uses the PEER NAG Strong Ground Motion Database to present a model of a high-speed railway with aballastless track and girder-bearing-pier-soil system under the influence of near-field and far-field seismic ground motions. The rail-wheel interactions and separations are modeled using the non-linear Hertzian contact theory. This paper uses a 32m, five-span PC girder bridge on the Beijing-Shanghai high-speed railway in China as a case study and examines how near-field ground motions influence the behavior of vehicles and the bridge.

2 DYNAMIC MODEL OF A COUPLED VEHICLE-BRIDGE SYSTEM

Figure 1 shows a coupled vehicle-bridge system, consisting of a bridge subsystem, a slab ballastless track system, and a train subsystem, subjected to near-field and far-field ground motions. The train runs over the bridge longitudinally and the train speed is assumed to remain constant. A global coordinate system is defined for the bridge-train system, in which the X-axis represents the longitudinal direction of the bridge, the Y-axis represents the lateral direction of the bridge, and the Z-axis represents the vertical direction following a right-hand rule.

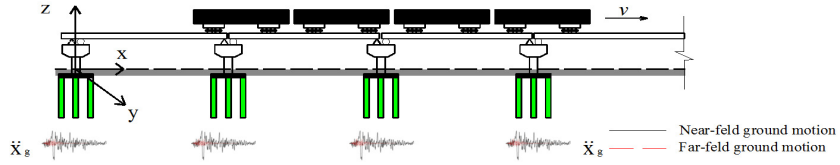

Figure 1. Model of train-bridge system under he influence of near-field and far-field ground motions

2.1 Vehicle subsystem

The train traveling on the bridge is composed of several motor and trailer cars moving at constant speed. Each vehicle is complicated multi-DOFs vibration system, with each system consisting of a car-body, bogies, wheel-sets, suspension springs and dashpots. The car-body, bogies and wheel-sets are rigid components. Each carbody or bogie has six DOFs to be concerned. They are designated by the lateral displacement Y_c , roll displacement θ_{xc} , yaw displacement ϕ_{zc} , vertical displacement Z_c , pitch displacement ψ_{yc} , and longitudinal displacement X_c , respectively. Each bogie has six DOFs designated by lateral displacement Y_t , roll displacement θ_{xt} , yaw displacement ϕ_{zt} , vertical displacement Z_t , pitch displacement ψ_{yt} , and longitudinal displacement X_t , respectively. For each wheel-set only five DOFs are considered: the lateral displacement Y_w , roll displacement θ_{xw} , yaw displacement ϕ_{zw} , vertical displacement

Z_w and longitudinal displacement X_w, respectively. Linear springs and viscous dashpots in both vertical and lateral directions represent both the connections between the car body and the bogies and the connections between the bogies and the wheel-sets. Therefore, a thirty-eight DOFs model can be established for a four-axle train car. The dynamic equilibrium of motion for the vehicle, with respect to its static equilibrium position, can be established in the following absolute coordinate system:

$$[M_V]\left\{\ddot{\delta}_V\right\}+[C_V]\left\{\dot{\delta}_V\right\}+[K_V]\{\delta_V\}=\{P_V\} \tag{1}$$

where M_V, C_V, and K_V denote the mass, damping, and stiffness matrices of the vehicle, respectively;

δ_V, $\dot{\delta}_V$ and $\ddot{\delta}_V$ are the displacement, velocity and acceleration vector of the vehicles respectively; P_V stands for the force vector on the vehicle.

2.2 Spatial vibration model of slab ballastless track structure

Figure 2 shows a new spatial vibration model of the ballastless slab track, established based on structural characteristics of the ballastless slab-track system.

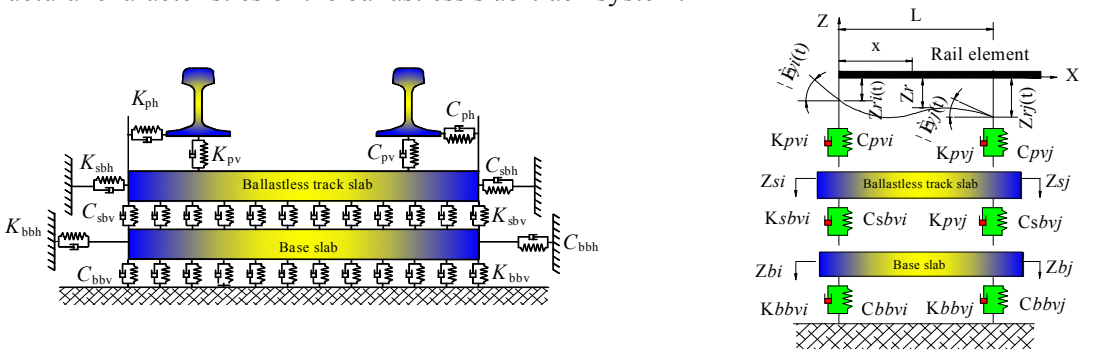

(a) Cross-section view **(b) Side ballastless slab track element**

Figure 2. Vibration model of ballastless slab track

This study uses the layered slab ballastless track CRTSⅡ (i. e., China Railway Track System Ⅱ Type Ballastless Slab Tracks). Each track element is placed between two adjacent fasteners. In each element, the rail consists of two-node, three-dimensional beams connected to concrete slabs with discrete visco-elastic supports every 0.625 m in the X-direction. The nodal displacement parameter takes in the rail at both sides. The fastener is replaced by a linear spring and a damp; the ballastless slab-track is a thin, elastic plate; and the nodal displacement parameter takes in the plate element at four vertices. A cement asphalt mortar (CAM) layer connects the ballastless slab-track to the concrete base slab. The CAM layer is a continuous-plane spring and a damp, and the concrete base slab is connected together with layered earthwork cloth. The vibration of the concrete base slab is a thin, elastic plate, and the nodal displacement parameter takes in the plate element at four vertices.

Figure 2(b) shows that, in the $X-Z$ coordinate plane, L is the distance between two adjacent fasteners, and according to the Hamilton principle, is the element stiffness matrix of the side rail-ballastless slab-track base element. Reference [6] shows the parameters of the ballastless track system. The damping, mass matrixes and nodal force column vector of the rail ballastless slab-track base element can be strengthened by applying the same method. Next, the FEM matrix equations of the triple-layered ballastless track system can be established by assembling the stiffness, damping, mass matrixes and the nodal force column vector of the element into the global matrixes.

2.3 Bridge subsystem

The bridge is represented by a three-dimensional finite element model in this study. Different components of the bridge can be modelled with beam elements. When a bridge supports a railway, tracks are laid on the bridge deck and force from the train wheels are transmitted to the bridge deck through the tracks. This study assumes that there is no relative displacement between the tracks and

the bridge deck. The elastic effects of the track system are also neglected. In the absolute coordinate system, the displacement vector of the bridge is divided into two parts: the displacement vector of the superstructure X_s, and the displacement vector of the bases X_b. Next, the equations of motion of the bridge can be expressed in partitioned form:

$$\begin{bmatrix} M_{ss} & M_{sb} \\ M_{sb}^T & M_{bb} \end{bmatrix} \begin{Bmatrix} \ddot{X}_s \\ \ddot{X}_b \end{Bmatrix} + \begin{bmatrix} C_{ss} & C_{sb} \\ C_{sb}^T & C_{bb} \end{bmatrix} \begin{Bmatrix} \dot{X}_s \\ \dot{X}_b \end{Bmatrix} + \begin{bmatrix} K_{ss} & K_{sb} \\ K_{sb}^T & K_{bb} \end{bmatrix} \begin{Bmatrix} X_s \\ X_b \end{Bmatrix} = \begin{Bmatrix} F_s \\ F_b \end{Bmatrix} \tag{2}$$

where M_{ss}, C_{ss}, and K_{ss} are the mass, damping, and stiffness matrices of the bridge superstructure; M_{bb}, C_{bb}, and K_{bb} represent the mass, damping, and stiffness matrices of the bridge bases; F_b is the reaction force vector acting on the bases of the bridge; F_s denotes the force vector on the bridge due to interaction between the bridge and train, The damping ratio of the bridge structure is assumed to be 3%, and is introduced into Equation (2) by using the Rayleigh Damping.

2.4 **dynamic interaction between wheel and rail**

The normal and tangential interaction force between wheel and rail can be obtained through the use of the non-linear, elastic Hertzian contact theory and through the use of Kalker linear theory. Calculating creeping forces with Kalker's linear theory may cause errors when a large creepage ratio exists. In such a case, the Shen-Hedrick-Elkins theory may be used to modify the linear theory.

The governing equations can be established by substituting Eqs. (1) and (2) into the wheel-rail relationship formulas with an iteration process. This study used the $Wilson-\theta$ method and the explicit integration method to find the best solution. TTBDA, a finite element program for the simulation of the dynamic responses of the coupled train-bridge system while subjected to earthquakes, has been developed based on the above formulations and MATLAB. This research considers the influence of the stiffness of the pot rubber bearing and of the soil-foundation interaction.

3 **NEAR-FIELD PULSE GROUND MOTION RECORDS**

A set of six pulse-like ground motion records were chosen to complement the near-field pulse ground motion database in Table 1, and therefore, to evaluate the seismic response of a high-speed railway vehicle-bridge system. Mw is the moment magnitude; Dis is the closest distance from the site to the fault rupture plane; A_H is an abbreviation for the horizontal peak ground acceleration (PGA); V_H is an abbreviation for horizontal peak ground velocity (PGV); and A_V is an abbreviation for the vertical PGA.

Table 1. Properties of near-field ground motions used in the analyses

Earthquake/ NGA no	Station	Dis/m	T_P/s	A_H/g	V_H/cm/s	A_V/g
Tabas, Iran 1978/0143	Tabas	1.79	6.19	0.85	121.4	0.69
Loma Prieta 1989/3548	Lexington Dam	3.22	2.40	0.44	62.1	0.15
Kocaeli, Turkey 1999/1176	Yarimca	1.38	4.95	0.35	62.1	0.24
Northridge 1994/1044	Fire Staion	3.16	1.37	0.59	97.2	0.54
Northridge 1994 /1063	Rinaadi	1.25	1.25	0.84	166.1	0.85
San Fernando 1971/0077	Pacoima Dam	1.64	1.64	1.23	112.5	0.57

The ground motions were mainly recorded with NEHRP soil type B (rock) and on soil type D (stiff soil) conditions. When a structure in two perpendicular directions is subjected to a near-field ground motion, the structure in one of the two directions will be subjected to excitations almost as severe as the fault-normal component. For this reason, this study focuses on the fault-normal component of near-field ground motions. From this point on, the horizontal ground motion component will be referred to as the rotated fault-normal (FN) one, and all of the vertical components of ground motions

will use physical records and will abandon the suggested value of two-thirds of the vertical-to-horizontal PGA ratio. The PEER NGA database contains all of the strong motion records. The period of the velocity pulse of the near-field ground motions in Table 3 are quantified from the dominant frequency of the extracted wavelet, according to the Reference [7]. The comparison of the seismic responses at near-field region sites to sites that are not influenced by the pulse effect is an important aspect of this study. Therefore, Table 2 uses a second set of far-field, nonpulse-like ground motions.

Table 2. Properties of far-fault ground motions used in the analyses

Earthquake/ NGA no	Station	Mw	Dis/km	A_H /g	V_H /cm/s	A_V /g
Tabas, Iran 1978/0140	Ferdows	7.3	89.76	0.108	8.6	0.053
Loma Prieta 1989 /0793	Cliff House	6.9	78.58	0.108	19.8	0.062
Kocaeli, Turkey 1999/1147	Ambarli	7.5	68.09	0.184	33.2	0.079
Northridge 1994 /0988	Century City	6.7	23.41	0.256	21.1	0.116
Loma Prieta 1989/0796	Presidio	6.9	77.34	0.099	12.9	0.058
Imperial Valley 1979/0162	Calexico	6.5	10.45	0.275	21.2	0.187

4 CASE STUDY

4.1 Bridge description and calculation parameters

The case study concerns a bridge on the planned Beijing-Shanghai high-speed railway in China. As Fig. 3 shows, the bridge is a typical five-span, simply-supported boxing bridge. The related parameters are a a pre-stressed concrete boxing girder spanning 32m, a round solid pier of 10-20 m, and a concrete strength grade of C35 for the piers. The Young's Modulus of the bridge girder is 3.02 E10N/m^2, and its Poisson's Ratio is 0.15. This study uses the Rayleigh Damping, and the damping ratio of the bridge structure is 3%. The rail is the CHN 60kg/m type supported on an upper slab ballastless track system with a support interval of 0.625 m in the rail direction. Figure 2 shows the concrete slab system, including a 20.0-cm-thick and25.5-cm-wide concrete ballastless track slab to support the rail, a 3.0-cm-thick CAM layer for cushioning, and a 20.0-cm-thick and 29.5-cm-wide concrete base slab to support the track structure on the bridge girders. The Young's Modulus and the Poisson's Ratio, for the concrete bed are 2E7 kN/m^2 and 0.2, those for the CAM layer are 3.0E8 kN/m^2 and 0.25, and those for the rail are 2E8 kN/m^2 and 0.3, respectively.

(a) Bridge deck (unit: mm) (b) Bridge pier (unit: cm)

Figure 3. Configuration of bridge deck and pier

The high-speed train used in this case study has 2 × 8 vehicles. The first, second, fourth, fifth, seventh, eighth, ninth, tenth, twelfth, thirteenth, fifteenth and sixteenth vehicles are motor cars, and the third, sixth, eleventh and fourteenth vehicles are trailer cars. Reference [6] lists the greatest parameters of the motor car and the trailer car. The train speeds used in calculation are 200-400 km/h atintervals of 20m/s. The speed used for the example in this case study was 350km/h . ANSYS software analyzed the natural vibration properties of the bridge. In total, thirty frequencies and mode shapes, corresponding to different damping ratios, were obtained for such a five-span bridge. The first lateral natural frequency was 2.4024 Hz and the first vertical natural frequency was 4.6815 Hz, with each measurement respectively corresponding to the lateral and vertical vibration of the main span. That is, the lateral fundamental period of the bridge is T_{s1}=0.42sec.

All records were scaled to match specific levels of ground motions. The maximum accelerations in the analysis were normalized as 0.2g (g = the acceleration of gravity), exactly equivalent to the so-called

Hazard level Ⅱ earthquake (Design Level Earthquake). Earthquakes at this hazard level are generally assumed to have a 10% chance of being surpassed in fifty years [8].

The in situ experiment on the SUI river extra-large bridge for the Beijing-Shanghai high-speed railway in China was carried out between 12-17 February 2011 in order to determine the dynamic behaviours of high-speed train-bridge systems and to verify an analytical model. Generally, when the train-bridge system model was used under high-speed train loading, the date measured in situ closely matched the calculated results, both in amplitudes and in distribution tendencies.

4.2 **Dynamic responses of the train-bridge system under seismic loads**

The near-field record of Tabas and the far-field record of Ferdows for Tabas during the 1978 Iran earthquake were used in this case study to analyze the seismic response of vehicle-bridge system, including the ballastless track system and the running safety of the vehicles. Figure 4 shows the seismic responses of the triple-layered ballastless track system when the train ran on the bridge at a constant speed of 350 km/h. It was demonstrated that great accelerations of the rail caused by near-field pulse-like motions sharply increase the impact between the wheel and the rail compared with effects of far-field or non pulse-like ground motions.

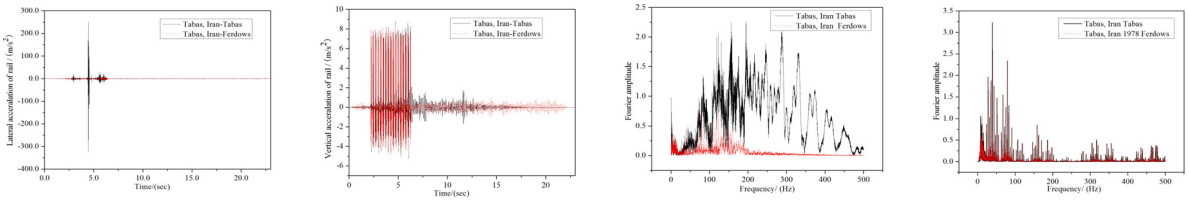

(a) Lateral acceleration of rail | (e) Vertical acceleration of rail | (k) Fourier spectrum of lateral acceleration of rail | (l) Fourier spectrum of vertical acceleration of rail

Figure 4. Seismic responses and Fourier spectrum of the rail for the vehicle-bridge system with 12m pier height, 32m span and 350km/h traveling speed

Figure 5 shows the seismic responses of the bridge structure, when the train ran on the bridge at a constant speed of 350 km/h. The results indicate that the time histories of lateral displacement and accelerations at the mid-span of the bridge reach maximum values earlier under near-field ground motion than under far-field ground motion. For vertical deflections and accelerations, the bridge begins to vibrate more intensely earlier under near-field ground motion than under far-field ground motion. As shown in Figure 5 (h), these results can be explained by the pulse-like effect of near-field ground motions, and can be associated with the spectrum characteristics of ground motions.

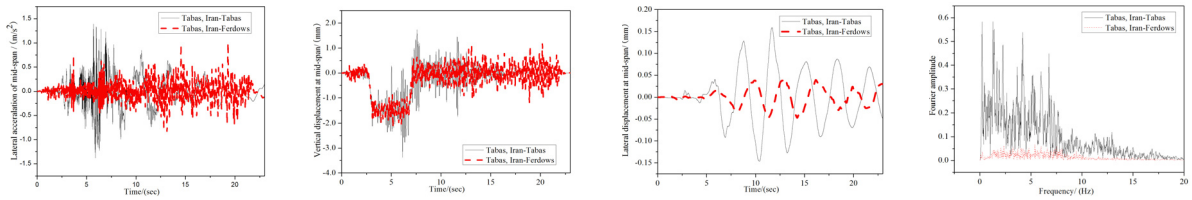

(a) Lateral acceleration of mid-span | (e) Vertical displacement of mid-span | (c) Lateral displacement of mid-span | (h) Fourier spectrum of ground motions

Figure 5. Seismic responses and Fourier spectrum of the bridge structure

For a short-period structure, such as the simply-supported boxing bridge in this study, $T_{SL} < 1.0\,\text{sec}$ and in the first-mode period-to-pulse ratio T_{SL} / T_P=0.24, 0.13, 0.30, 0.13, and 0.34≤ 0.35 [9]. However, for the short period bridge, as Figures 5(a), 5(b) and 5(c) demonstrate, lateral and vertical displacement and acceleration at mid-span of girder are greater under near-field ground motions than under far-field records during the same earthquake.

The evaluation indices for the running safety of train vehicles currently adopted for high-speed railways in China include: the derailment factor Q/P (defined as the ratio of the lateral wheel-rail force to the vertical wheel-rail force); the offload factor $\Delta P/P$ (defined as the ratio of the offload vertical wheel-rail force to the static lateral wheel/rail force); the lateral wheel-rail force Q; and the

lateral and vertical acceleration of carbody as represented by a_y and a_z [10].

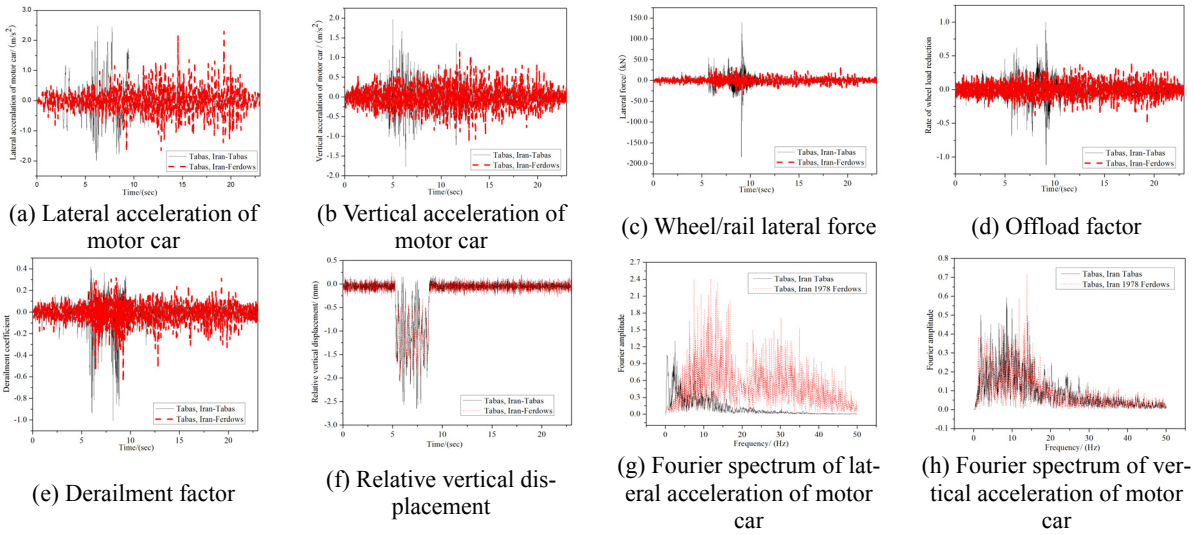

(a) Lateral acceleration of motor car

(b Vertical acceleration of motor car

(c) Wheel/rail lateral force

(d) Offload factor

(e) Derailment factor

(f) Relative vertical displacement

(g) Fourier spectrum of lateral acceleration of motor car

(h) Fourier spectrum of vertical acceleration of motor car

Figure 6. The seismic responses of the vehicles in the vehicle-bridge system with 12m pier height, 32m span and 350km/h traveling speed

As shown in Figs. 6(a) and 6(b) , far-field ground motion delays the peak response time, compared with the far-field input, of lateral and vertical acceleration responses of the car body. These results are compatible with the Fourier spectrum of lateral acceleration and vertical acceleration of motor car as shown in Figs. 6(g) and 6(h). Figs. 6(c), 6(d) and 6(e) show the wheel/rail lateral force, the offload factor and the derailment factor. As can be seen, the indices for the running safety are characterized by visible pulse-like effects. Table 3 shows that, much more than far-field ground motions, near-field ground motions significantly influence the running safety of trains because of their pulse-like effect.

Table 3. Seismic peak values of the vehicle in the vehicle-bridge system with 12m pier height, 32m span and 350km/h traveling

Earthquake	a_y /m/s^2	a_z /m/s^2	Q /kN	$\Delta P / P$	Q / P
Tabas, Iran 1978 Tabas	2.4827	1.9633	69.604	0.9516	1.3037
Tabas, Iran 1978- Ferdows	2.3032	1.1448	35.658	0.4967	0.8590
Loma Prieta 1989- Lexington Dam	8.7729	0.6927	48.252	4.2318	1.1421
Loma Prieta 1989- Cliff House	0.9126	0.5552	64.329	0.9548	1.7039
Kocaeli, Turkey 1999- Yarimca	1.3794	2.0953	40.945	0.5145	1.1447
Kocaeli, Turkey 1999- Ambarli	0.4982	0.6474	22.386	0.3515	0.3575
Northridge 1994- Fire Staion	4.6633	2.2139	69.514	0.9336	0.8629
Northridge 1994- Century City CC	2.0596	0.8213	40.348	0.5718	0.9179
Northridge 1994- Rinaadi	0.5205	0.4264	56.202	0.5034	2.1600
Loma Prieta 1989- Presidio	1.1415	0.6367	65.552	0.8022	1.3989
San Fernando 1971- Pacoima Dam	4.0040	1.4258	37.041	2.1561	2.3320
Imperial Valley 1979- Calexico	2.4853	1.7501	76.857	0.8199	3.0394

The nonlinear Hertzian contact model used in this study allows the separation between the wheels and the rails of the coupled train-bridge system to be investigated, which is crucial for train safety evaluation. Figure 6(f) shows the relative vertical displacement between the right wheel of the eighth wheel-set (of the second motor car) and the rail. The negative value shows the wheel jumping on the rail. There is an interesting dynamic motion of both wheels alternately jumping, due to the resonant rolling effects of the body, truck and wheel-set caused by the near-field pulse-like ground motions.

5 CONCLUSIONS

This study establishes a dynamic model for a coupled train-bridge system subjected to near-field and far-field ground motions, in which rail-wheel interactions and possible separations between the wheels

and the rails are considered through the non-linear contact between the wheels and the rails. The major conclusions drawn from the case study are as follows:

(1) The lateral/vertical displacement and the acceleration of the triple-layered ballastless track system, the mid-span of the girder and the top of the pier increase more under near-field ground motions than under far-field records during the same earthquake. The lateral acceleration of the rail caused by the impact of pulse-like motions on the wheel and rail increases most significantly.

(2) In terms of the dynamic response of train vehicles, the lateral car body accelerations, derailment factors, offload factors and lateral wheel-rail forces all increase under near-field ground motions. Because the pulse-like effects of near-field ground motions more significantly impact the running safety of train vehicles, the influences of near-field ground motions should be taken into account in evaluating the running safety of vehicles on bridges during earthquakes.

(3) Compared with far-field ground motions, near-field ground motions cause greater lateral/vertical acceleration car body responses and make the peak response time occur earlier. As the peak response time of an earthquake generally is in the previous stage of the earthquake's history, an earlier peak response may lead to more serious effects from the earthquake and may increase the risk of derailment.

6 ACKNOWLEDGEMENTS

The research summarized in this paper was supported by the China Postdoctoral Science Foundation through Grant No. 2013M530022, the Science and Technology Plan Projects of Ministry of Housing and Urban-Rural Development of the People's Republic of China through Grant No. 2013-K5-31, the High-level Scientific Research Foundation for the introduction of talent from Yangzhou University, and the Open Fund of the National Engineering Laboratory for High Speed Railway Construction.

REFERENCES

Yang, Y.B. and Wu, Y.S. 2002. Dynamic stability of trains moving over bridges shaken by earthquakes. *Journal of Sound and Vibration*, 258(1): 65-94.

Xia, H. Han, Y. Zhang, N. and Guo W.W. 2006. Dynamic analysis of train-bridge system subjected to non-uniform seismic excitations. *Earthquake Engineering and Structural Dynamics,* 35(12): 1563-1579.

Du, X.T. Xu, Y.L. and Xia, H. 2011. Dynamic interaction of bridge–train system under non-uniform seismic ground motion. *Earthquake Engineering and Structural Dynamics,* 41(1): 139-157

Miyamoto, T. Ishida, H. and Matsuo, M. 1997. Running safety of railway vehicles as earthquake occurs. *Report of RTRI,* 38(3):117-122.

Chen, L. K. Jiang L. Z. and Yu, Z.W. 2013. Influence of ballastless track constraint on the seismic responses of high-speed railway train-bridge system. *Chinese Journal of Computational Mechanics,* 30(6): 763-769 (in Chinese)

Chen, L. K. Seismic responses of high-speed railway train-ballastless track-bridge system and train-running safety during earthquake. Doctoral dissertation, Changsha: China, Central south university, 2012. (in Chinese)

Baker. J. W. 2007, Quantitative classification of near-fault ground motions using wavelet analysis. *Bulletin of the Seismological Society of America,* 97(5): 1486-501.

FEMA-356. *Prestandard and commentary for seismic rehabilitation of buildings.* Washington DC: Federal Emergency Management Agency, 2000.

Babak, Alavi. and Helmut, Krawinkler. 2004. Behavior of moment-resisting frame structures subjected to near-fault ground motions. *Earthquake Engineering and Structural Dynamics*, 33(6): 687-706.

TB10621-2009. *Code for design of high speed railway.* Beijing: China, China railway Publishing House, 2010. (in Chinese)